

## Level positions of interstitial transition-metal impurities in silicon

Gary G. DeLeo, George D. Watkins, and W. Beall Fowler

*Department of Physics, Lehigh University, Bethlehem, Pennsylvania 18015*

(Received 7 December 1981)

The single-donor and single-acceptor level positions associated with defect- to band-state excitations are calculated for the interstitial transition-metal impurities V, Cr, Mn, Fe, Co, and Ni in silicon. Electronic relaxation and many-electron corrections are included. The single-particle electronic structures have been calculated by us previously according to the self-consistent-field scattered-wave  $X\alpha$  cluster method, and reported in earlier papers. The effects of electronic relaxation are here estimated by the Slater transition-state procedure. Many-electron corrections are considered in two approximations: A spin-unrestricted approach which includes only spin-induced correlation between electrons, and an approach suggested by Hemstreet and Dimmock which includes both space- and spin-induced correlations between electrons, but in an approximate way. The level positions computed using the latter approximation scheme are in good agreement with experiment with the possible exceptions of the Fe single-acceptor level and the V single-donor level. It is found that the many-electron corrections to the computed level positions are relatively small ( $\sim 0.1$  eV) provided that the effect is properly included in both the initial and final states. Electronic relaxation is found to separate single-donor and single-acceptor levels by  $\sim 0.3$  eV.

### I. INTRODUCTION

We extend here our previous treatments of the interstitial iron-group transition-metal impurities to include electron and hole excitations to the band edges. The results of our spin-restricted electronic structure calculations on the interstitial Cr, Mn, Fe, Co, and Ni impurities in silicon were reported in an earlier publication<sup>1</sup> (hereafter referred to as I). In the preceding paper<sup>2</sup> (hereafter referred to as II), the treatment of I was extended to include many-electron effects and the set of impurities considered was extended to include vanadium. We showed in II that, with many-electron effects properly included, the computed results supported the ground-state spin and symmetry identifications (Hund's rule) for the neutral interstitial impurities previously made on the basis of electron-paramagnetic-resonance (EPR) experiments.<sup>3</sup> A set of excited terms within the  $d^n$  manifold was generated as well for each of the impurities V, Cr, Mn, and Fe. Transitions between these terms (ground and excited) correspond to single-particle excitations within the crystal-field-split  $d$ -like states in the band gap; i.e., the internal transitions ( $d^n \rightarrow d^n$ ). These excitations have not been observed in silicon.

Another class of excitations involves the promotion of an electron to the conduction band ( $d^n \rightarrow d^{n-1} + \text{conduction electron}$ ), or a hole to the valence band ( $d^n \rightarrow d^{n+1} + \text{valence hole}$ ). The total energy difference between the states of the system before and after such an excitation defines the donor or acceptor electrical level position with respect to the corresponding band edge. Although EPR can provide impurity charge-state, spin, and symmetry identifications, it cannot easily locate the electrical level positions. Deep-level transient capacitance spectroscopy (DLTS) on the other hand can estimate these level positions directly, and several such studies have been reported recently for the interstitial transition-metal impurities in silicon.<sup>4,5</sup> It is these excitations which we consider in this paper.

In I and II, electronic relaxation was included in the ground manifold of states ( $d^n$ ) by self-consistently computing the electronic structure for each configuration (electron occupancy scheme) separately. In II, many-electron effects were then introduced, further splitting this manifold of states into terms. The lowering of the ground-term energies, although considerably smaller than the free-atom energy lowerings, was found to be significant ( $\sim 0.4$  eV) when compared with the band gap of

silicon ( $\sim 1.2$  eV). Therefore, in order to properly locate the electrical levels relative to the band edges, it is clearly necessary to include these same effects, electronic relaxation and many-electron energy lowerings, not only in the initial state but in the final state as well, where an electron (hole) has been promoted to the conduction- (valence-) band edge.

An outline of the present paper is as follows: In Sec. II, we consider the *single-particle* states in the spin-restricted and spin-unrestricted pictures, the latter including many-electron effects in an approximate way. Periodic trends in the level positions are estimated from these single-particle results. The effects of electronic relaxation on the level positions are considered in Sec. III A and, in an alternative approximation, many-electron effects are included in Sec. III B. This alternative approach to the many-electron effects suggested by Hemstreet and Dimmock<sup>6</sup> may be described as an approximate configuration mixing within the  $d^n$  manifold of states. Both methods of introducing the many-electron energy were discussed in the preceding paper (II). A discussion is presented in Sec. IV and a summary in Sec. V.

## II. SINGLE-PARTICLE DESCRIPTION

Our model for the interstitial environment is provided by the cluster  $\text{Si}_{10}\text{H}_{16}$ , centered at the high-symmetry ( $T_d$ ) interstitial position.<sup>1,2</sup> The transition-metal atoms are successively placed at the origin, and the single-particle electronic structures are calculated by the self-consistent-field scattered-wave  $X\alpha$  method.<sup>7-11</sup> Hydrogen atoms, which serve to terminate the cluster by tying up the dangling bonds,<sup>12-14</sup> have been placed at two different sets of positions reflecting two different Si-H bond lengths: Cluster *A* denotes the cluster with Si-H distance equal to the normal crystalline Si-Si distance; cluster *B* has this distance reduced by 25%. As discussed in II, the motivation for considering these two clusters is that they have complimentary deficiencies. Our cluster *A* provides extended states near the band edges to which the impurity  $3d$  states may readily couple; it also gives a reasonable "band gap." Cluster *B* gives a more realistic representation of the local bonding at the expense of extended-state couplings.

The spin-restricted single-particle states of interest are shown in Figs. 1(a) and 1(b) for clusters *A* and *B*, respectively. The electrically active defect states located in the gap are labeled  $5t_2$  and  $2e$

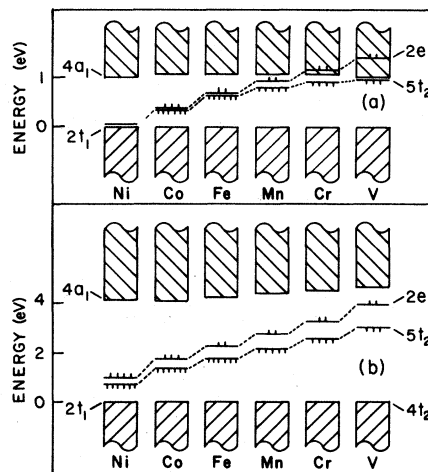


FIG. 1. Single-particle spin-restricted electronic structures for the  $\text{Si}_{10}\text{H}_{16}$  cluster with transition-metal impurities at the center. The Si-H distances are equal to (a) the crystalline Si-Si distance (cluster *A*) and (b) 75% of the crystalline Si-Si distance (cluster *B*).

in the figures. The filled  $2t_1(4t_2)$  and empty  $4a_1$  states represent the valence- and conduction-band edges, respectively, in our model systems. The defect states ( $5t_2, 2e$ ) are about twice as localized on the impurity for cluster *B* than for cluster *A*, leading to a more rapid increase in these single-particle energy-level positions for cluster *B* as the impurity atomic number decreases. The periodic trends, however are similar for clusters *A* and *B* and, although these single-particle defect states do not represent electrical level positions, they do provide us with a useful approximation to them.

Many-electron or correlation energy may be readily introduced in an approximate way while still retaining the single-particle orbitals. This is accomplished by relaxing the restriction which requires spin-up and spin-down components of a given single-particle state to have the same spatial form and experience the same potential.<sup>8,9</sup> These spin-unrestricted calculations were reported by us in II. The results are reproduced here in Fig. 2, but for cluster *B* only; we have been unable to achieve self-consistency for spin-unrestricted calculations which use cluster *A*.

The single-particle electronic structures of Fig. 2 provide the following useful information at a glance: (i) The predicted ground-state spin assignments follow naturally from the occupation of these single-particle states from lowest to highest energy; i.e., Hund's-rule (high-spin) occupancies are predicted in all cases, in agreement with experi-

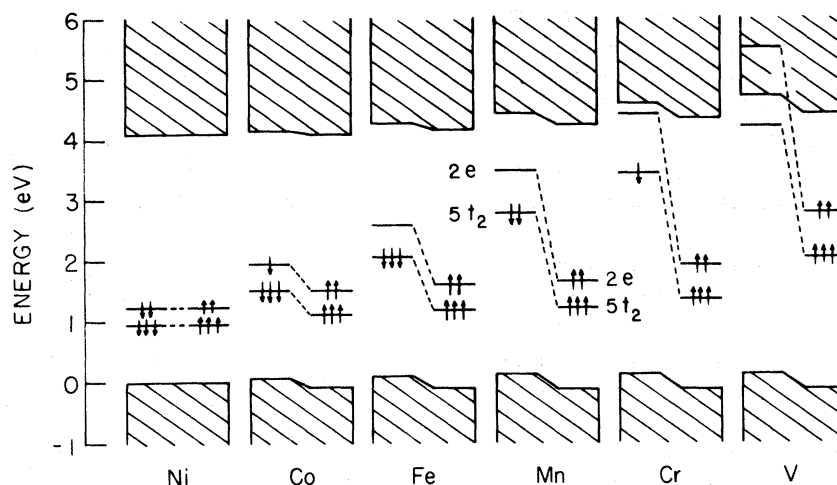


FIG. 2. Single-particle spin-unrestricted electronic structures for the  $\text{Si}_{10}\text{H}_{16}$  cluster with transition-metal impurities at the center. The Si-H distance is 75% of the crystalline Si-Si distance (cluster B).

ment. (ii) Periodic trends in electron (hole) excitation energies and hence, in donor (acceptor) level positions, can be estimated by considering the energy difference between the state containing the most weakly bound electron (hole) and the conduction-(valence-) band edge. (iii) Many-electron corrections to the level positions can be estimated by considering the spin-up and spin-down energy shifts from their centers of gravity ( $\sim$ spin-restricted values). For example, the Cr donor level is raised; the V donor level is lowered.

Since the single-particle electronic structures of Fig. 2 do not contain final-state (after excitation) electronic relaxations, justification of statement (ii) is required. We find by the methods described in the following section that the electronic relaxation energies are typically  $\sim 0.25$  eV for cluster B and  $\sim 0.15$  eV for cluster A. This means that the single-donor (acceptor) levels are nearer to the valence (conduction) band by about these amounts relative to what is estimated from the single-particle picture. What makes statement (ii) valid, however, is that these energies are relatively constant throughout the transition-metal series; hence, the single-particle electronic structures still provide us with meaningful trends in the level positions in going from one element to the next.

Consider, therefore, the set of impurity atoms Fe, Mn, Cr, and V. The most weakly bound electrons for Fe, Mn, and Cr, and the most weakly bound holes for Mn, Cr, and V may be readily identified with the minority-spin ( $\downarrow$ )  $5t_2$  state. The smooth monotonic rise in this single-particle state ( $5t_{2\uparrow}$ ) in going backwards through the transition-metal series predicts therefore a similar rise in the

corresponding single-donor (Fe, Mn, Cr) and single-acceptor (Mn, Cr, V) levels. From (iii), we note that this rise is more rapid than it would be in the absence of many-electron effects.

Similar considerations indicate that we may expect breaks in this smooth periodic trend at the endpoints since the Fe acceptor hole comes from the higher energy minority-spin ( $\downarrow$ )  $2e$  state (raised by the crystal field), while the V donor electron comes from the lower energy majority-spin ( $\uparrow$ )  $2e$  state (raised by the crystal field, but lowered more by many-electron effects).

Quantitative considerations of Fig. 2 indicate that not only are the absolute excitation energies too large when compared with the true band gap of silicon ( $\sim 1.2$  eV), but so are the relative excitation energies; e.g., the Fe and Cr electron excitation energies differ by  $\sim 1.5$  eV for cluster B. The relative excitation energies are a measure of defect-wave-function localization on the transition-metal impurities. Therefore, the computational results suggest that the defect wave function is too localized in cluster B. Another measure of localization is the effective electron-electron interaction energy  $U$ , here defined as the difference in energy between the donor and acceptor levels for a single impurity, when the corresponding electron and hole excitations derive from the same single-particle state. From Fig. 2 this is the case for the donor-acceptor energy difference for Mn. This energy, estimated by the methods described in the following section, is found to be  $\sim 0.5$  eV for cluster B (approximately twice the relaxation energy for either electron or hole excitations). This is larger than the experimental value for Mn of  $\sim 0.3$  eV, again indicating

too much localization for cluster *B* calculations.

It may be possible to scale the results of Fig. 2 (cluster *B*) so that they would be appropriate to a reduced degree of localization, thereby providing quantitative as well as qualitative level positions. Such a scaling was discussed in II. We choose not to pursue this approach here; instead, we consider cluster *A*.

Our electronic structure calculations on cluster *A* give defect-state charge localizations which are about half of those generated by cluster *B*. In the following section, we consider the cluster *A* electronic structure calculations. Electronic relaxation is considered explicitly and level positions are computed but in the absence of many-electron effects in Sec. III A. These level positions are then corrected for many-electron effects in an alternative approximation scheme in Sec. III B.

### III. LEVEL POSITIONS

The position of the single-donor level, denoted  $(0/+)$ , relative to the conduction-band edge is defined as the difference in total energy between the relaxed ground state of the neutral defect and the relaxed state in which a single electron has been promoted to the conduction-band edge. The relaxation referred to includes both electronic and lattice relaxation. This energy difference is denoted  $E(0/+)$ . The position of the single-acceptor level, denoted  $(-/0)$ , relative to the valence-band edge is similarly defined except that here we refer to hole excitation to the valence band rather than electron excitation to the conduction band. This energy difference is denoted  $H(-/0)$ . The double donor  $(+/++)$  and double acceptor  $(=-/-)$  are also similarly defined where here the excitations are from the singly charged states. Therefore, if the Fermi level is located between the single-acceptor  $[(-/0)]$  and single-donor  $[(0/+)]$  levels, then the defect will be present in the neutral charge state. If the Fermi level is located between  $(0/+)$  and  $(+/++)$ , then the defect will be present in the positive charge state, etc.

#### A. Electronic relaxation

The partially occupied states of Figs. 1 and 2 do not represent level positions since the electronic relaxations associated with the final states (after excitation) have not been included. In the absence of many-electron effects and lattice relaxation, the

computed energy difference between the conduction-band edge and the single-donor level  $[E(0/+)]$  for Mn, for example, is properly the energy difference between the configurations  $\cdots (5t_2)^5(2e)^2(4a_1)^0$  and  $\cdots (5t_2)^4(2e)^2(4a_1)^1$ , where both are electronically relaxed. The former configuration contains the high-spin term of the neutral defect; the latter contains that of the singly ionized impurity. In a similar manner, the energy of the single-acceptor level relative to the valence-band edge  $[H(-/0)]$  is the energy difference between the configurations  $\cdots (2t_1)^6(5t_2)^5(2e)^2$  and  $\cdots (2t_1)^5(5t_2)^6(2e)^2$ . In a case such as this where the most weakly bound electron and hole both come from the same single-particle state, it is electronic relaxation which brings about the difference in the single-donor and single-acceptor level positions. This difference  $U$  vanishes for transitions not accompanied by electronic relaxation.<sup>15</sup>

In this paper, we estimate these energy differences by Slater's transition-state method.<sup>8</sup> Accordingly, the energy  $E(0/+)$  for Mn is the energy difference between the single-particle levels  $5t_2$  and  $4a_1$  where the calculation is carried out self-consistently for the intermediate ("transition-state") configuration which is  $\cdots (5t_2)^{4.5}(2e)^2(4a_1)^{0.5}$ . The  $4a_1$  state is clearly not a true conduction-band state since we have only a finite cluster; however, it is quite delocalized over the cluster and should reproduce the conduction-band edge sufficiently well for our purposes. Similarly for the state  $2t_1$ , we expect a reasonable representation of the valence-band edge. In order to test this, we have promoted the electron to a Watson sphere surrounding the cluster instead of to the  $4a_1$  state and then carried out the same calculation. The results for  $E(0/+)$  were very nearly the same by either method.

Although it is known from experiment that there are no static Jahn-Teller (symmetry-lowering) distortions for these ions, a dynamic Jahn-Teller coupling may be expected for ground terms with electronic degeneracy.<sup>3</sup> A symmetrical ( $A_1$ ) distortion also may be present. In our treatment we include neither of these effects, which are assumed to contribute only small changes in the energies.

The computed single-donor  $[(0/+)]$  and single-acceptor  $[(-/0)]$  levels for Fe, Mn, Cr, and V, appropriate to spin-restricted cluster *A* electronic structures, are shown in Fig. 3. The recent DLTS observations of Graff and Pieper<sup>4</sup> are also shown in the figure. It is readily seen that those computed levels which involve electron or hole excitations from the  $5t_2$  state (Fe, Mn, Cr donors; Mn, Cr ac-

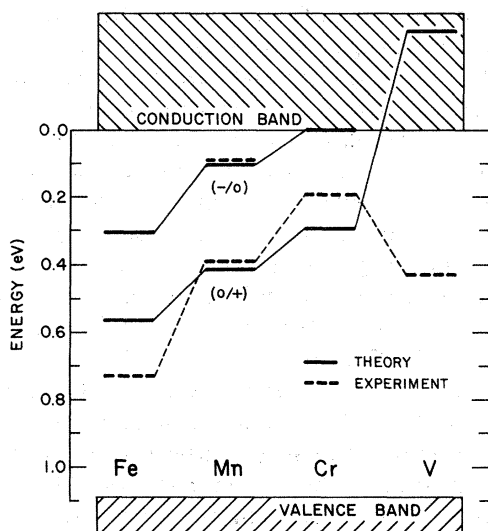


FIG. 3. Single-donor [(0/+)] and single-acceptor [(-/0)] level positions computed for cluster *A* in the absence of many-electron effects. Shown for comparison are experimental results determined by DLTS (Ref. 4; dashed lines). The placement of a "single-donor level" in the conduction band means that the computed neutral  $d^n$  charge state is predicted to be unstable. The DLTS values are shown scaled down by 1.09/1.16 to conform to our computed band gap of 1.09 eV.

ceptors) are in rather good agreement with experiment. The computed donor-acceptor energy difference for Mn,  $U \sim 0.3$  eV, is also in good agreement with experiment. Disagreement appears to exist, however, between the theory and experiment for those levels which involve excitations from the  $2e$  state, namely, the Fe acceptor level (for which there is no experimental evidence) and the V donor level. A more subtle difference between theory and measured single-donor levels is present in the rate at which these levels move up in going from Fe to Cr.

The predicted stable charge states include  $\text{Fe}^+$ ,  $\text{Fe}^0$ ,  $\text{Fe}^-$ ,  $\text{Mn}^+$ ,  $\text{Mn}^0$ ,  $\text{Mn}^-$ ,  $\text{Cr}^+$ , and  $\text{Cr}^0$ . This is fully consistent with the EPR results, with the exception of  $\text{Fe}^-$  for which there is no EPR evidence.<sup>16</sup>

### B. Many-electron corrections

In addition to being split by the crystal field, the transition-metal  $d^n$  configurations are further split by the many-electron interaction. The high-spin ground terms which correspond to  $d^n$  of  $X^0$  [ $d^n(X^0)$ ] and  $d^{n-1}$  of  $X^+$  [ $d^{n-1}(X^+)$  with one electron promoted to the conduction band], where  $X$  runs from V to Ni, are all lowered in energy

when many-electron effects are included. If the lowest energy term of  $d^{n-1}(X^+)$  is lowered more than that of  $d^n(X^0)$ , then the single-donor level will be raised in the band gap relative to that calculated in the absence of many-electron effects. In this case, the final state, which is higher in energy, is lowered more by many-electron effects than the initial state; therefore, the total energy required to excite the electron to the conduction-band edge is reduced. Conversely, the single-donor level is lowered in the band gap if the ground term of  $d^n(X^0)$  is lowered more by many-electron effects than that of  $d^{n-1}(X^+)$ . Similar reasoning may be applied to the acceptor levels as well.

A method for estimating the term splittings, and therefore the energy lowering of the high-spin term due to many-electron effects, has been developed by Hemstreet and Dimmock<sup>6</sup> (referred to in II as the "matrix method"). The electron-electron interaction  $1/r_{12}$  is included perturbatively, thereby mixing spin-restricted crystal-field configurations formed by populating the partially occupied  $e$  and  $t_2$  defect gap states. The required two-electron matrix elements are estimated by scaling down atomic Racah parameters<sup>17</sup> according to defect-state ( $e, t_2$ ) localization on the transition-metal impurity as computed by the scattered-wave  $X\alpha$  method. The  $A$  Racah parameter effectively subtracts out the already present spherically symmetric potential according to Ref. 6. The energies which separate interacting configurations are estimated by the Slater transition-state method.<sup>8</sup> Here, our term-splitting procedure differs somewhat from that of Hemstreet and Dimmock since they use uniformly spaced configurations. The matrix elements of  $1/r_{12}$  have been conveniently tabulated by Sharma, de A. Viccaro, and Sundaram<sup>18</sup>; we use these tabulated values. Further details may be found in Ref. 6 and in II.

To illustrate our procedure, let us consider in detail the many-electron correction to the Fe single-donor level position appropriate to cluster *A*. The spin-restricted scattered-wave  $X\alpha$  method provides the relative configurational energies and the Hemstreet-Dimmock scaling factors  $R_{ee}$  and  $R_{tt}$  which are here defined as the fractional  $d$ -like charges in the impurity region (sphere) for the states  $2e$  and  $5t_2$ , respectively. These parameters have been reported by us for  $d^8(\text{Fe}^0)$  in II. For  $d^7(\text{Fe}^+)$ , the scaling factors  $R_{ee}$  and  $R_{tt}$  computed for the high-spin configuration  $(5t_2)^5(2e)^2$  are 0.346 and 0.241, respectively; the computed energies which separate the configurations  $(5t_2)^6(2e)^1$ ,  $(5t_2)^5(2e)^2$ ,  $(5t_2)^4(2e)^3$ , and  $(5t_2)^3(2e)^4$  are, in eV,

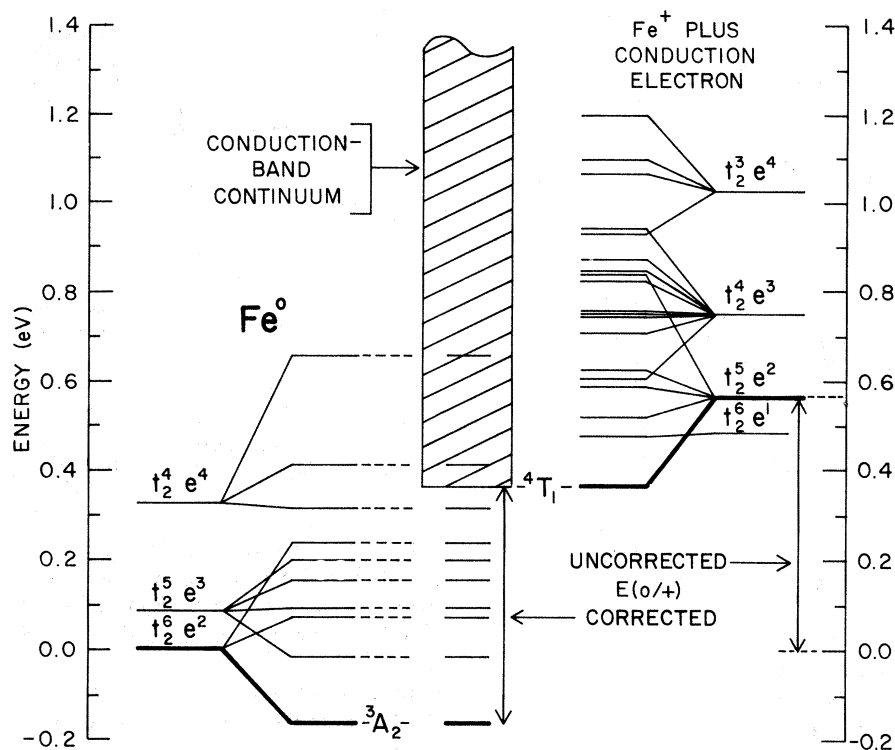


FIG. 4. Term structures of  $\text{Fe}^0$  (left) and  $\text{Fe}^+$  (right; one electron has been promoted to the lowest unoccupied cluster state  $4a_1$  which represents our "conduction-band edge" for cluster  $A$ ). In the absence of many-electron effects, the single-donor level position relative to the conduction-band edge is the energy difference between the configurations  $\cdots (5t_2)^6(2e)^2$  and  $\cdots (5t_2)^5(2e)^2$ . When corrected for many-electron effects, this becomes the difference between the terms  ${}^3A_2$  and  ${}^4T_1$ , as shown.

0.083, 0.183, and 0.274, respectively. In these calculations, the cluster was kept neutral, the promoted electron being placed in the  $4a_1$  state; i.e.,  $d^7$  means  $d^7(4a_1)^1$ . The computed  $d^8(\text{Fe}^0)$  and  $d^7(\text{Fe}^+)$  term structures, shown in Fig. 4, are located relative to one another by setting the energy difference between the configurations  $(5t_2)^6(2e)^2$  of  $\text{Fe}^0$  and  $(5t_2)^5(2e)^2$  of  $\text{Fe}^+$ , equal to  $E(0/+)$  as calculated in the absence of many-electron effects (Fig. 3; Sec. III A). The corrected level position is now the energy difference between the  ${}^4T_1$  term of  $\text{Fe}^+$  and the  ${}^3A_2$  term of  $\text{Fe}^0$ . Also, all of the  $\text{Fe}^0$  terms which are higher in energy than the  ${}^4T_1$  term of  $\text{Fe}^+$  are now seen to be resonances in the continuum.

This procedure has been applied to the interstitial Mn, Cr, and V impurities as well. The  $(R_{ee}, R_{tt})$  scaling factors are (0.410, 0.307), (0.430, 0.335), and (0.405, 0.334) for  $\text{Mn}^+$ ,  $\text{Cr}^+$ , and  $\text{V}^+$ , respectively. The corresponding term splittings for  $\text{Mn}^0$ ,  $\text{Cr}^0$ , and  $\text{V}^0$  have been reported in II.

The computed changes in the Fe, Mn, Cr, and V single-donor level positions are shown in Fig. 5

along with the corresponding contributions from the initial- and final-state energy lowerings. It is clear that the magnitude of the many-electron effect on level positions is sizeably reduced when it is properly included in both initial and final states. We believe that this point has not been made in any previous publication. From the figure, it is seen that (i) the magnitude of the correction increases with increasing spin, and (ii) the sign depends on whether the removal of an electron increases or decreases the defect spin. These many-electron corrections exhibit the same qualitative features as those inferred from the spin-unrestricted treatment; e.g., comparison of Figs. 1(b) and 2 show many-electron effects at a glance.

The calculated single-donor and single-acceptor levels corrected for many-electron effects are shown in Fig. 6 along with DLTS results.<sup>4</sup> The primary effect of this correction has been to increase the rate at which the single-donor levels move up in going from Fe to Cr, and to lower the V single-donor level, which still remains, however, in the conduction band. The conduction-band continuum begins at energies  $E(0/+)$  above the ap-

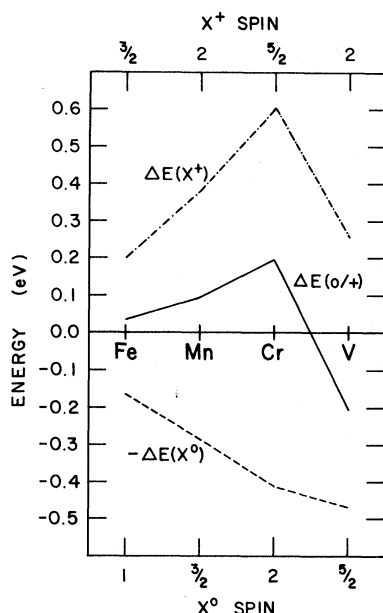


FIG. 5. Many-electron energy lowerings of high-spin terms of neutral [ $\Delta E(X^0)$ ] and singly ionized [ $\Delta E(X^+)$ ] impurities for cluster *A*. The difference [ $\Delta E(0/+)$ ] represents the many-electron correction to the computed level position. A positive many-electron correction is defined so as to move  $(0/+)$  nearer to the conduction band.

appropriate ground terms. Therefore, excited terms for  $\text{Fe}^0$ ,  $\text{Mn}^0$ , and  $\text{Cr}^0$  which are above the corresponding ground terms by more than 0.53, 0.32, and 0.10 eV, respectively, are actually resonances in the conduction-band continuum (see Figs. 6–8 in II).

#### IV. DISCUSSION

The cluster *A* results with many-electron corrections shown in Fig. 6 are, aside from a uniform shift, in remarkably good agreement with experiment for those levels which involve electron or hole excitations from the  $5t_2$  state (Fe, Mn, Cr single donors; Mn, Cr single acceptors). Many-electron corrections are seen to have improved the agreement with experiment. The cluster *B* spin-unrestricted calculations on the other hand give a rate of increase for the Fe through Cr single-donor level positions and an effective electron-electron interaction energy  $U$  (donor-acceptor energy separation for Mn), which are too large. Since these quantities are related to the defect wave-function localization on the transition-metal atom, we tentatively conclude that our cluster *A* provides the more realistic degree of localization, where here

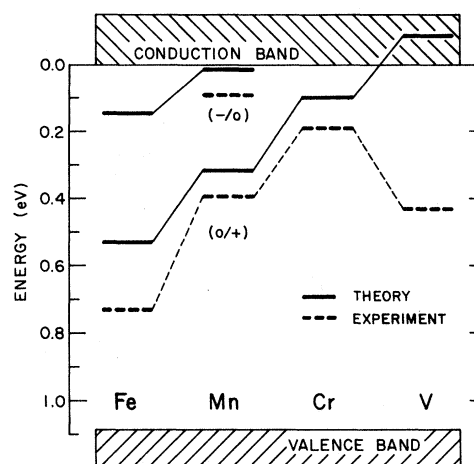


FIG. 6. Single-donor  $[(0/+)]$  and single-acceptor  $[(-/0)]$  level positions computed for cluster *A* including many-electron effects. Shown for comparison are experimental results determined by DLTS (Ref. 4; dashed lines). The placement of a “single-donor level” in the conduction band means that the computed neutral  $d^n$  charge state is predicted to be unstable. The DLTS values are shown scaled down by 1.09/1.16 to conform to our computed band gap of 1.09 eV.

~35% of the defect-state charge is on the transition-metal impurity.

We note that the cluster *A* spin-restricted electronic structures for neutral Cr and V [Fig. 1(a)] have as a common feature an occupied  $2e$  state which is higher in energy than the unoccupied  $4a_1$  state. Superficially it might have seemed therefore from this single-particle representation that the ionized impurities should have a lower energy than their neutral counterparts (i.e.,  $d^{n-1}4a_1$  lower than  $d^n$ ). Of course this is not necessarily so since electronic relaxation and many-electron effects have not yet been included. In fact, we have seen that for Cr, inclusion of these effects lowers the ground term of the neutral impurity [ $d^6(^5T_2)$ ] below that of the singly ionized impurity [ $d^5(^6A_1)$ ] by the excitation energy  $E(0/+)$  as indicated in Fig. 6. The many-electron “forces” which stabilize the  $\text{Cr}^0 d^6$  high-spin term relative to that of  $d^5(4a_1)^1$  do not win out in the case of V, however, as shown in Fig. 6 where the single-donor state “ $(0/+)$ ” is predicted to be above the conduction-band edge. Therefore, our calculations do not predict a stable  $d^5(^6A_1)$  ground state for neutral V, but instead we presumably have a localized  $d^4$  core and a weakly bound (effective-mass-like) electron as the ground state; i.e.,  $d^4(4a_1)^1$ . Hence, our model predicts a

shallow single-donor level [excitation of  $d^4(4a_1)^1$ ] and presumably a deeper second-donor level (excitation of  $d^4$ ). The presence of a deep second-donor level could be consistent with EPR,<sup>3</sup> and also with DLTS (Ref. 4) provided that the observed level (Fig. 6) is identified as the second-donor level, with the shallow single-donor level not yet observed.

On the other hand, the spin-unrestricted cluster *B* calculations (Fig. 2) clearly suggest a downward jog in the single-donor level associated with V, since for this cluster, the many-electron energy substantially exceeds the crystal-field energy for V. This model therefore supports the identification of the observed V level as a single-donor level. If this is correct, it means that with cluster *A* we have overestimated the crystal-field energy relative to the many-electron energy for V. The DLTS level identification is only tentative and the EPR observation of  $V^{2+}$  is consistent with either model. Therefore, at present we cannot decide between the two possibilities which is correct. A critical and important experiment in resolving this would be an EPR study of the neutral V impurity since a deep  $d^5$  impurity state if present should be easily observed.

There is strong evidence from EPR that the negative charge state of Fe is not stable.<sup>16</sup> Our cluster *A* results predict a stable  $Fe^-$  impurity with or without many-electron effects. If the experimental observations are correct, it would seem that we are underestimating the crystal-field splitting at Fe. It is clear from Fig. 1(a) that the calculated value for this quantity is small. We have argued in I that the computed crystal-field splitting at Fe may be anomalously low as a consequence of our small cluster which has so few *e* states. A similar line of reasoning might explain an overestimate of the crystal-field splitting at V.

As we have pointed out earlier, electron-lattice effects are not considered in this treatment. If they are present, however, and are sizeably different between initial and final states, then further corrections to our computed level positions would be necessary.

## V. SUMMARY

We have illustrated how to calculate donor- and acceptor-level positions including electronic relaxation and many-electron effects. Electronic relaxation separates the computed donor and acceptor levels. Many-electron effects lower the energies of

both initial and final (ionized) states, but by different amounts, thereby giving rise to a correction to the predicted excitation energies.

The interstitial transition-metal impurities have been simulated by two clusters: Cluster *A* emphasizes  $3d$  coupling to extended states near the band edges; cluster *B* provides a better representation of local bonding at the expense of these extended-state couplings. Our cluster *A* with many-electron effects, previously shown to predict the Hund's-rule ground states observed by EPR,<sup>2</sup> is here shown to give a reasonable treatment of single-donor and single-acceptor level positions. The Mn donor-acceptor energy separation *U* is found to be  $\sim 0.3$  eV. The initial- and final-state many-electron energy lowerings are found to be sizeable. However, since the correction is determined by the difference in energy lowerings, it is not as large as might have been expected, but still  $\sim 0.1$  eV. The agreement between our cluster *A* model and experiment (DLTS) (Ref. 4) for *U* and the relative single-donor level positions suggests that the predicted defect-state localization ( $\sim 35\%$  of defect-state charge on impurity) is reasonable.

The *e*-state excitations may not be handled as well in our model as evidenced by the prediction of stable interstitial  $Fe^-$ , contrary to EPR observations.<sup>16</sup> The single-particle *e* state may be sensitive to cluster size and termination, perhaps leading us to underestimate the crystal-field energy at Fe. The V impurity donor levels also involve *e*-state excitations. Our cluster *A* calculations predict a shallow single-donor level and suggest a deep second-donor level for the V impurity. If on the other hand we have exaggerated the crystal-field energy relative to the many-electron energy at V, then presumably we would predict a deep single-donor level. This latter interpretation is consistent with the present and still tentative identification of a deep V single-donor level using DLTS (Ref. 4) and also with our cluster *B* prediction.

The overall results are quite good, encouraging future work with the cluster-*A*-type models and the Hemstreet-Dimmock<sup>6</sup> approach to many-electron effects.

## ACKNOWLEDGMENTS

The authors are grateful to the Lehigh University Computing Center for the generous amount of computer time and assistance which was made available. This research was supported by the U.S. Navy ONR Electronics and Solid State Science Program Contract No. N00014-76-C-1097.



- <sup>1</sup>G. G. DeLeo, G. D. Watkins, and W. B. Fowler, Phys. Rev. B **23**, 1851 (1981).
- <sup>2</sup>G. G. DeLeo, G. D. Watkins, and W. B. Fowler, Phys. Rev. B, preceding paper **25**, 4962 (1982).
- <sup>3</sup>G. W. Ludwig and H. H. Woodbury, in *Solid State Physics*, edited by F. Seitz and D. Turnbull (Academic, New York, 1962), Vol. 13, p. 263.
- <sup>4</sup>K. Graff and H. Pieper, in *Semiconductor Silicon 1981* (Electrochemical Society, Pennington, New Jersey, 1981), Vol. 81-5, p. 331.
- <sup>5</sup>L. C. Kimerling, J. L. Benton, and J. J. Rubin, in *Defects and Radiation Effects in Semiconductors, 1980*, edited by R. R. Hasiguti (Institute of Physics, London, 1981), p. 217.
- <sup>6</sup>L. A. Hemstreet and J. O. Dimmock, Phys. Rev. B **20**, 1527 (1979).
- <sup>7</sup>K. H. Johnson and F. C. Smith, Jr., Phys. Rev. B **5**, 831 (1972).
- <sup>8</sup>J. C. Slater, *The Self-Consistent Field for Molecules and Solids* (McGraw-Hill, New York, 1974).
- <sup>9</sup>K. H. Johnson, in *Advances in Quantum Chemistry*, edited by P. O. Löwdin (Academic, New York, 1973), Vol. 7, p. 143.
- <sup>10</sup> $X\alpha$  computer program written by F. C. Smith, Jr. and K. H. Johnson, MIT, Cambridge, MA.
- <sup>11</sup>K. Schwarz, Phys. Rev. B **5**, 2466 (1972).
- <sup>12</sup>B. G. Cartling, J. Phys. C **8**, 3171 (1975).
- <sup>13</sup>B. G. Cartling, J. Phys. C **8**, 3183 (1975).
- <sup>14</sup>L. A. Hemstreet, Phys. Rev. B **15**, 834 (1977).
- <sup>15</sup>In the context of an electronic transition, the "electronic relaxation" energy is here taken as the energy difference between properly computed excitation energies (total energy differences) and the corresponding single-particle energy differences, *as determined from our local-density ( $X\alpha$ ) calculations*. We make this point because the physical interpretation of the *single-particle states* is different for the local-density theory employed here than, say, for Hartree-Fock theory. It follows therefore that "electronic relaxation" has a meaning which depends on the electronic-structure method employed. In any scheme, however, what we ultimately want and in fact calculate are the total energy differences, which have a more universal meaning. For a more complete discussion of this point, see Ref. 8.
- <sup>16</sup>E. Weber (private communication).
- <sup>17</sup>J. S. Griffith, *The Theory of Transition-Metal Ions* (Cambridge University Press, London, 1961).
- <sup>18</sup>R. R. Sharma, M. H. de A. Viccaro, and S. Sundaram, Phys. Rev. B **23**, 738 (1981); **23**, 6855 (1981).